Bioorganic Chemistry 87 (2019) 688–698

Contents lists available at ScienceDirect

Bioorganic Chemistry

journal homepage: www.elsevier.com/locate/bioorg

# Sanggenon O induced apoptosis of A549 cells is counterbalanced by protective autophagy

Zhong-Rui Li[1], Ting Ma[1], Yan-Jia Guo, Bo Hu, Sheng-Hui Niu, Feng-Zhi Suo, Lin-Na Du, Ying-Hua You, Wen-Ting Kang, Shuan Liu, MAA Mamun, Qi-Meng Song, Jing-Ru Pang, Yi-Chao Zheng*, Hong-Min Liu*

*Collaborative Innovation Center of New Drug Research and Safety Evaluation, Henan Province, PR China*
*Key Laboratory of Advanced Drug Preparation Technologies (Zhengzhou University), Ministry of Education of China, PR China*
*Key Laboratory of Henan Province for Drug Quality and Evaluation, PR China*
*School of Pharmaceutical Sciences, Zhengzhou University, Zhengzhou 450001, PR China*

ARTICLE INFO

*Keywords:*
Sanggenon O
Non-small cell lung cancer
Cell proliferation
Autophagosome
Apoptosis

ABSTRACT

Sanggenon O (SO) is a Diels-Alder type adduct extracted from *Morus alba*, which has been used for its anti-inflammatory action in the Oriental medicine. However, whether it has regulatory effect on human cancer cell proliferation and what the underlying mechanism remains unknown. Here, we found that SO could significantly inhibit the growth and proliferation of A549 cells and induce its pro-apoptotic action through a caspase-dependent pathway. It could also impair the mitochondria which can be reflected by mitochondrial membrane permeabilization. Besides, SQSTM1 up-regulation and autophagic flux measurement demonstrated that exposure to SO led to autophagosome accumulation, which plays a protective role in SO-treated cells. In addition, knocking down of LC3B increased SO triggered apoptotic cell rates. These results indicated that SO has great potential as a promising candidate combined with autophagy inhibitor for the treatment of NSCLC. In conclusion, our results identified a novel mechanism by which SO exerts potent anticancer activity.

## 1. Introduction

Lung cancer remains a significant cause of mortality globally, being the first leading cause of cancer-related deaths in China, which accounts for 18% of deaths among cancer patients [1,2]. Among all lung cancer cases, non-small cell lung cancers (NSCLCs) accounts for 85% of deaths [3]. Lung cancer is often diagnosed at advanced stages, when local therapies and surgery are no longer effective, leading to poor survival outcomes in most settings. Therefore, chemotherapy is one of the most common therapies in many cases. However, the available lung cancer chemotherapeutic drugs perform extensive side-effects such as alopecia, hypocytosis and mucositis [4]. Therefore, it is necessary to develop more effective and safer drugs for the treatment of lung cancers, especially for NSCLCs.

Sanggenon O (SO, Fig. 1A), a flavanone Diel-Alder adduct compound, is isolated from the root bark of *Morus alba* [5], which is known for its anti-asthma and diuretic effects. Besides, extracts of *Morus alba* were also reported to possess some other biological and pharmacological activities, such as antidiabetic [6,7], anti-inflammatory [8,9], antioxidant [10], antihyperlipidemia [11], cardioprotective [12], and anti-cancer activities [13,14]. However, the biological activity of SO on human NSCLC cells has not been studied.

Apoptosis, as the most well characterized programmed cell death (PCD), usually exhibits as caspases-dependent accompanied with morphological feature changes including cell shrinkage, plasma membrane blebbing, chromatin condensation, DNA fragmentation and formation of apoptotic bodies [15]. Autophagy, a highly conserved process, could eliminate unnecessary or damaged cytoplasmic contents in cellular microorganisms in a lysosome-dependent manner [16]. Apoptosis and autophagy are both important in normal physiology and in a variety of diseases such as cancers, Parkinson and myocardial ischemia. Currently, in the process of cancer treatment, agents which induce cell

*Abbreviations:* SQSTM1, sequestosome 1; LC3B, microtubule-associated protein 1 light chain 3 beta; SO, Sanggenon O; MTT, 3-(4,5-dimethylthiazol-2-yl)-2, 5-diphenyltetrazolium bromide; EdU, 5-ethynyl-20-deoxyuridine; MDC, monodansylcadaverine; PBS, phosphate-buffered saline; PAGE, polyacrylamide gel; CQ, chloroquine; Baf, bafilomycin A1

* Corresponding authors at: School of Pharmaceutical Sciences, Zhengzhou University, Zhengzhou 450001, PR China.
*E-mail addresses:* yichaozheng@zzu.edu.cn (Y.-C. Zheng), liuhm@zzu.edu.cn (H.-M. Liu).
[1] These authors contributed equally to this work.

https://doi.org/10.1016/j.bioorg.2019.03.072
Received 3 January 2019; Received in revised form 28 February 2019; Accepted 27 March 2019
Available online 04 April 2019
0045-2068/ © 2019 Published by Elsevier Inc.

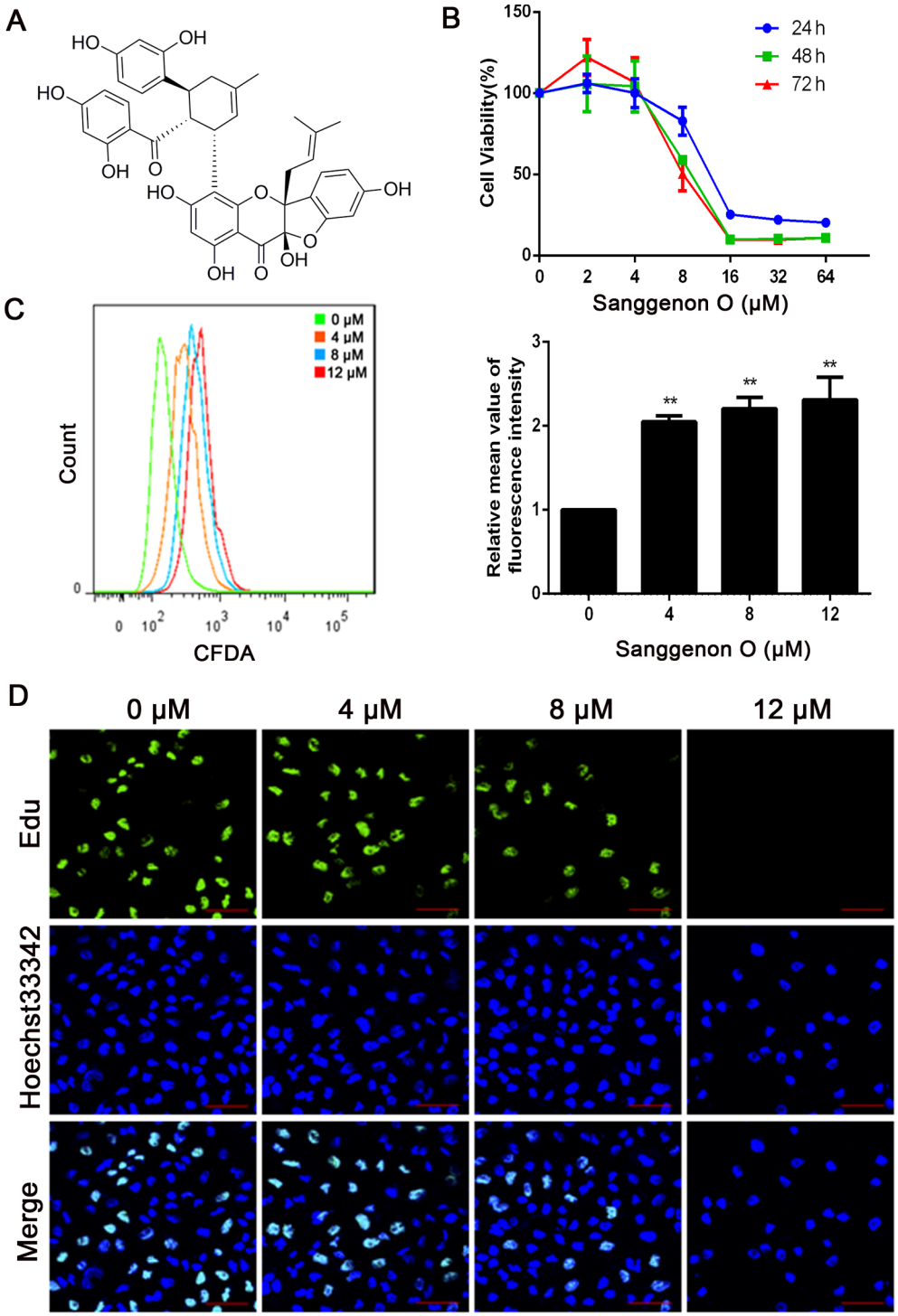


**Fig. 1.** Sanggenon O inhibits A549 cell proliferation. (A) Chemical structure of SO. (B) Cell viability assay in A549 cells. Cells were treated with a series of concentrations of SO (0–64 μM) for 24 h, 48 h or 72 h, then the cell viability was measured via an MTT assay at each indicated time point. (C) After exposing to different concentrations of SO (0–12 μM) for 48 h, A549 cells were collected for CFDA-SE staining assay. (D) EdU staining assay was performed after A549 cells pretreated with various concentrations of SO for 48 h. Cells were observed and images were taken by a confocal microscopy. Bar = 100 μm. Data are presented as mean ± SD of triple independent experiments. $^{**}p < 0.01$, compared to control.

apoptosis are mainly used. Mitochondrion plays a major role in cell apoptosis. Therefore, inducing mitochondrial dysfunction is an effective way for cancer treatment. In addition, there are two opposite conclusions about the relationship between apoptosis and autophagy. On one side, autophagy protects cancer cells to adapt to environmental pressures during their growth and metastasis; on the other side, autophagy contributes to apoptosis. Therefore, it is of significant importance to look for apoptosis-targeted drugs and elucidate the relationship between autophagy and apoptosis in the treatment of cancers.

Here, we evaluated the anti-proliferative and autophagy flux inhibition effect of SO on human NSCLC cell line and explored the relationship between SO induced apoptosis and autophagy. Our results suggest that SO exhibits anti-cancer effects by inducing apoptosis and SO may be used as a promising anticancer agent for the treatment of NSCLC.

## 2. Materials and methods

### 2.1. Reagents and chemicals

SO (purity > 98%) was purchased from Jisskang Biotechnology Company (Qingdao, China) and prepared as a bulk solution at 50 mM in DMSO (Sigma Aldrich, USA). Autophagy inhibitors (CQ, Baf and pepstatin A/E64d) were purchased from Beyotime Biotechnology

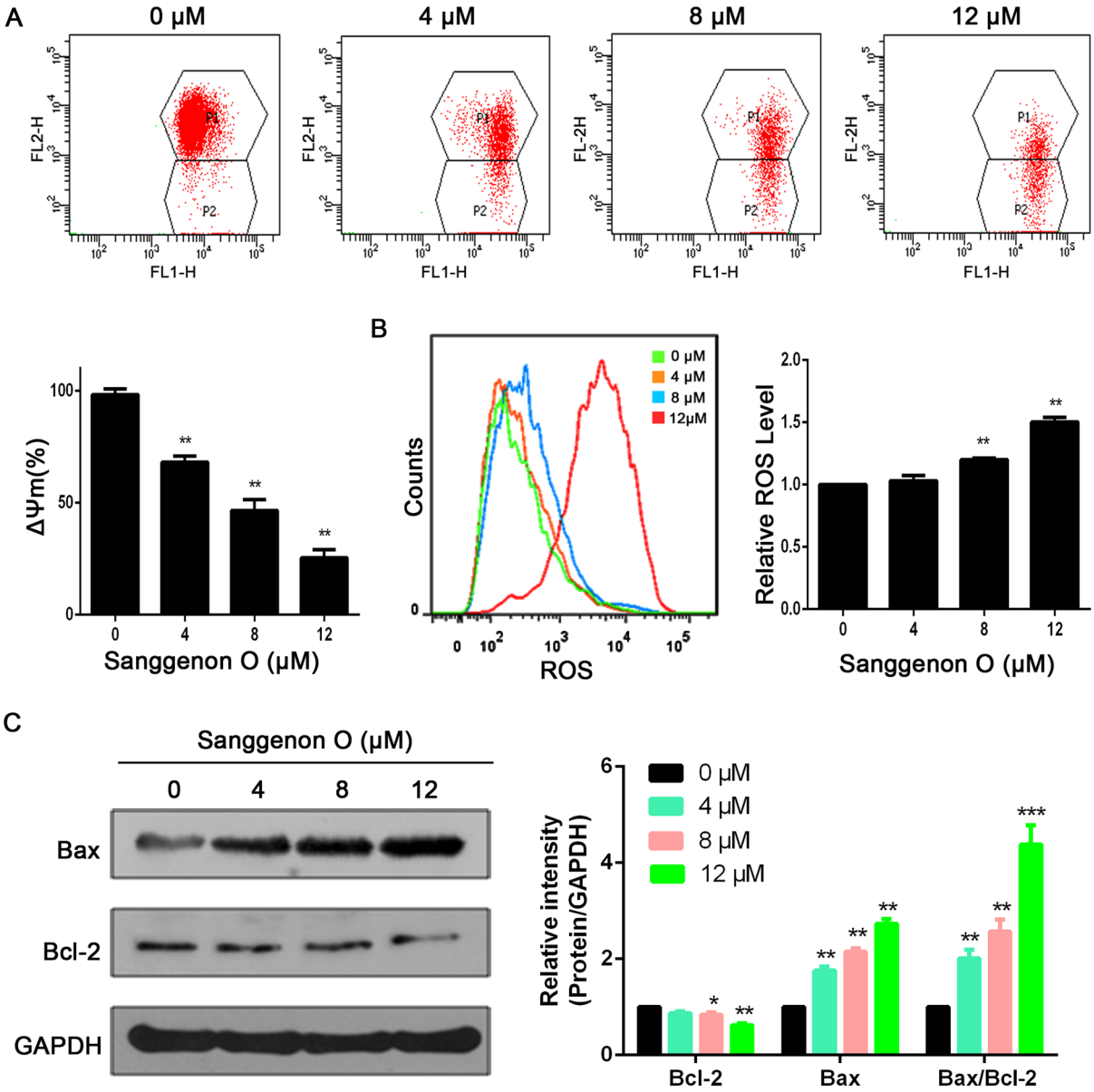


**Fig. 2.** Sanggenon O induces mitochondrial dysfunction in human lung cancer A549 cells. (A) After treatment with SO (0–12 μM) for 48 h, mitochondrial membrane potentials of the A549 cells was detected by flow cytometry after JC-1 staining. (B) After treatment with SO (0–12 μM) for 48 h, ROS was measured by flow cytometry with fluorescent dye DCFH-DA. (C) After treatment with SO (0–12 μM) for 48 h, the expressions of Bcl-2 and Bax were detected by western blot. Data are presented as mean ± SD from triple independent experiments. $^{*}p < 0.05$; $^{**}p < 0.01$ and $^{***}p < 0.001$, compared to control.

(Shanghai, China). MTT was purchased from Solarbio Technology Company (Beijing, China). Antibodies of cleaved caspase-3, cleaved caspase-7, cleaved caspase-9, cleaved PARP, caspase-3, caspase-7, caspase-9, PARP, LC3B and SQSTM1 were purchased from Cell Signaling Technology (Danvers, MA, USA). Antibodies of Bax and Bcl-2 were purchased from EnoGene Technology Company (Nanjing, China). GAPDH was purchased from Goodhere Biotechnology Company (Hangzhou, China). Peroxidase-conjugated affinipure goat anti-rabbit secondary antibody was purchased from Origene Technology Company (Beijing, China). The siRNAs were purchased from Genepharm (Shanghai, China). The sequence of siRNA for LC3B and SQSTM1 are: CACCUUCGAACAAAGAGUAdTdT, CCAUCCAGUAUUCAAAGCA dTdT.

### 2.2. Cell culture

A549 cells were purchased from the Cell Bank of Shanghai Institute of Biochemistry and Cell Biology, Chinese Academy of Sciences (Shanghai, China). A549 cells were cultured in RPMI-1640 media with 10% FBS at 37 °C in 5% $CO_2$.

### 2.3. Cell viability assay

The cell viability was measured via MTT assay. Cells were transferred in 96-well plates at a density of $3 \times 10^3$ cells per well. Following incubation overnight, cells were treated with a series of concentrations of SO for 24, 48 and 72 h. Then, 20 μL of MTT solution (5 mg/mL) was added into each well and incubated for 4 h. The supernatant was then removed and 150 μL of DMSO (Sigma Aldrich, USA) was added to dissolved formazan crystals. The absorbance was evaluated at 490 nm using a microplate reader.

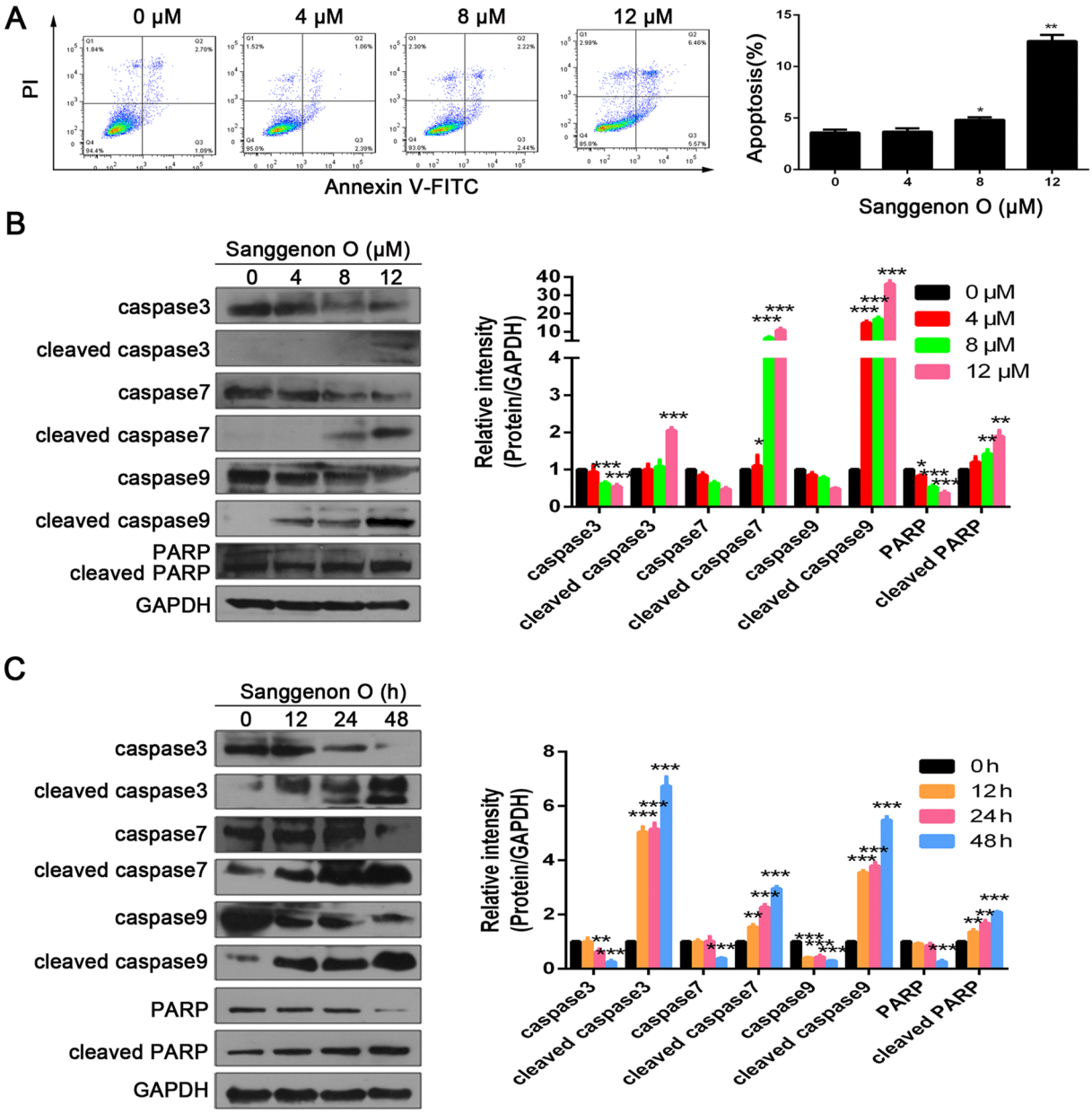


**Fig. 3.** Sanggenon O induces apoptosis in human lung cancer A549 cells. (A) A549 cells were pretreated with SO (0–12 μM) for 48 h, and apoptosis rates were determined by flow cytometry with Annexin V-FITC (AV) and PI stains. (B and C) After treatment with SO (0–12 μM) for 48 h or SO (8 μM) for different time (0–48 h), the expressions of caspase-9, cleaved caspase-9, caspase-3, cleaved caspase-3, caspase-7, cleaved caspase-7, PARP, and cleaved PARP were determined by Western blot. GAPDH served as a loading control for both western blots. Data are represented as mean ± SD of triple independent experiments. $^{*}p < 0.05$; $^{**}p < 0.01$ and $^{***}p < 0.001$, compared to control.

### 2.4. CFDA-SE cell tracer assay

Cell proliferation was detected by the CFDA-SE kit (Beyotime, China). Briefly, A549 cells were incubated with CFDA-SE, and seeded in six-well culture plates. After incubation for 24 h, medium was discarded and replaced with fresh medium containing SO at different concentrations (4–12 μM) or DMSO (< 0.1%) as a vehicle. The cells were harvested after 48 h, and the fluorescence intensity was measured by flow cytometry (BD Bioscience, USA).

### 2.5. 5-Ethynyl-20-deoxyuridine (EdU) incorporation assay

According to the instruction of EdU labeling/detection kit (Ribobio, China), cells were incubated in a final volume of 1 mL of complete medium at $3 \times 10^3$ cells per confocal laser dish (Corning Incorporated, USA). After incubation overnight, medium was removed and replaced with fresh medium containing different concentrations (4–12 μM) of SO or DMSO as a vehicle (< 0.1%). 48 h later, EdU labeling agent (50 μM) was added to the cell culture medium and incubated for 2 h at 37 °C in presence of 5% $CO_2$. Next, cells were fixed with 4% paraformaldehyde (pH 7.4) for 30 min and incubated with glycine for 5 min. After washing with PBS, cells were treated with anti-EdU working solution at 25 °C for 30 min. Cells were then stained with 5 μg/mL Hoechst33342 at 25 °C for 30 min after washing with 0.5% TritonX-100 in PBS. Finally, the cells were observed with a confocal laser scanning microscope.

### 2.6. Flow cytometry analysis of apoptosis

Cell apoptosis was detected by flow cytometry after double staining cells with fluorescein isothiocyanate labeled Annexin V (FITC-AV) and

Propidium iodide (PI) (KeyGEN BioTECH, China) in accordance with the instructions. Briefly, cells were harvested prior to resuspension in 500 μL of binding buffer. Then, FITC-AV (5 μL) was added to the sample. Next, PI (10 μL) was added to the mixture before further incubation at 25 °C for 5–15 min avoiding light, followed by flow cytometry analysis within 1 h.

### 2.7. Proteins extraction and western blotting

A549 cells were treated with DMSO (< 0.1%) or various concentrations (4, 8, and 12 μM) of SO for 48 h, then the cells were harvested and lysed in RIPA lysis buffer with protease inhibitors. Bicinchoninic acid protein (BCA) assay kit (Beyotime, China) was used to determined protein concentration. Equal weight protein from the total cell lysates (30–40 μg/lane) was separated on (8%, 12% or 15%)

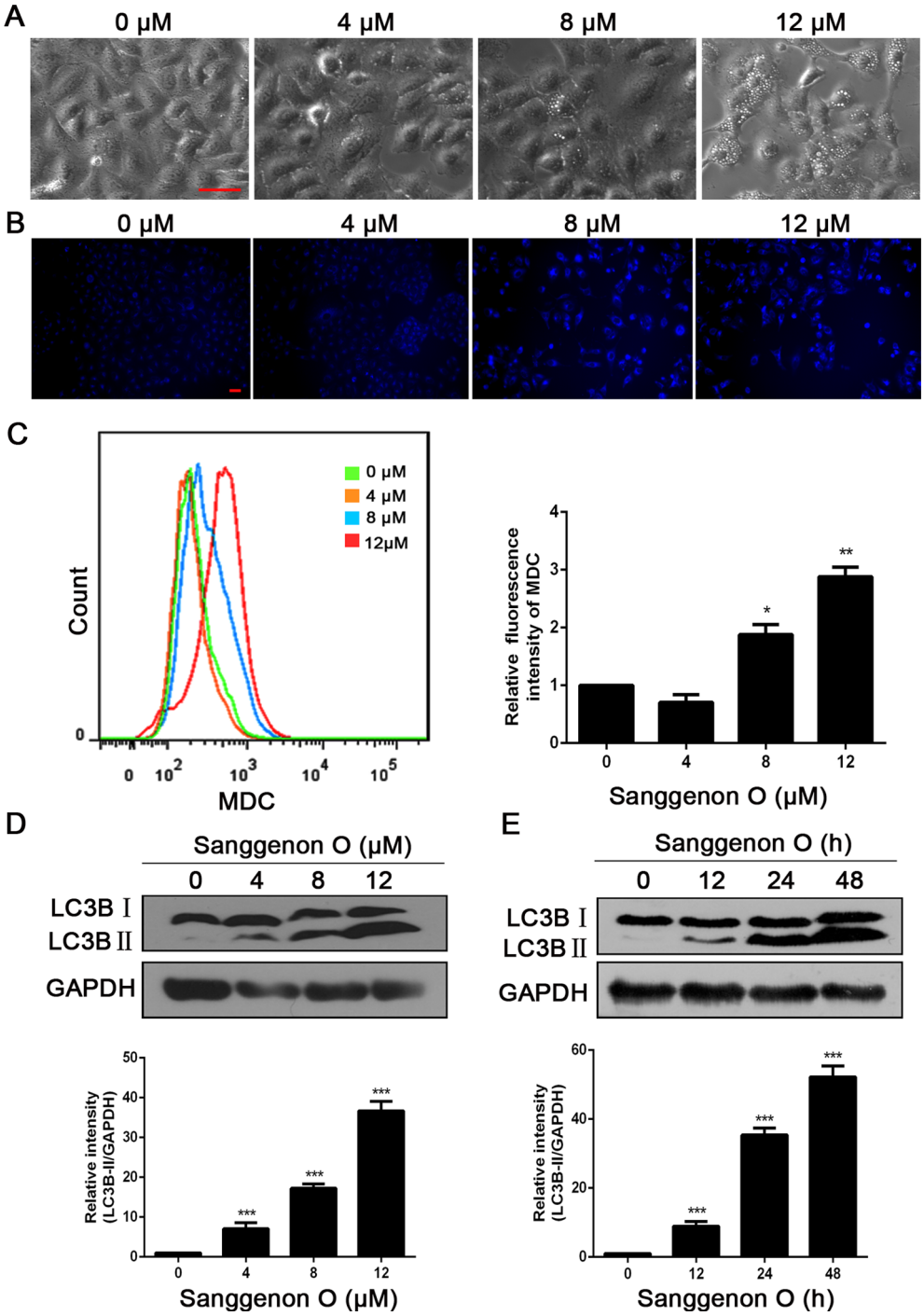


**Fig. 4.** Sanggenon O induces autophagosome accumulation in A549 cells. (A) After pretreated with SO (0–12 μM) for 48 h, the formation of cytoplasmic vacuoles in A549 cells was obtained under an inverted microscope. Bar = 50 μm. (B and C) After treatment with SO (0–12 μM) for 48 h, MDC staining was measured by fluorescence microscope (10 magnification) and flow cytometry. Bar = 15 μm. (D and E) After treatment with SO (0–12 μM) for 48 h or SO (8 μM) for various durations (0–48 h), the expression of LC3B-II was analyzed by western blot. (F) Accumulation of LC3B puncta in A549 cells was measured by immunofluorescence in cells treated with SO (4–8 μM) for 48 h. Bar = 30 μm. Data are represented as mean ± SD of triple independent experiments. $^{*}p < 0.05$; $^{**}p < 0.01$ and $^{***}p < 0.001$, compared to control.

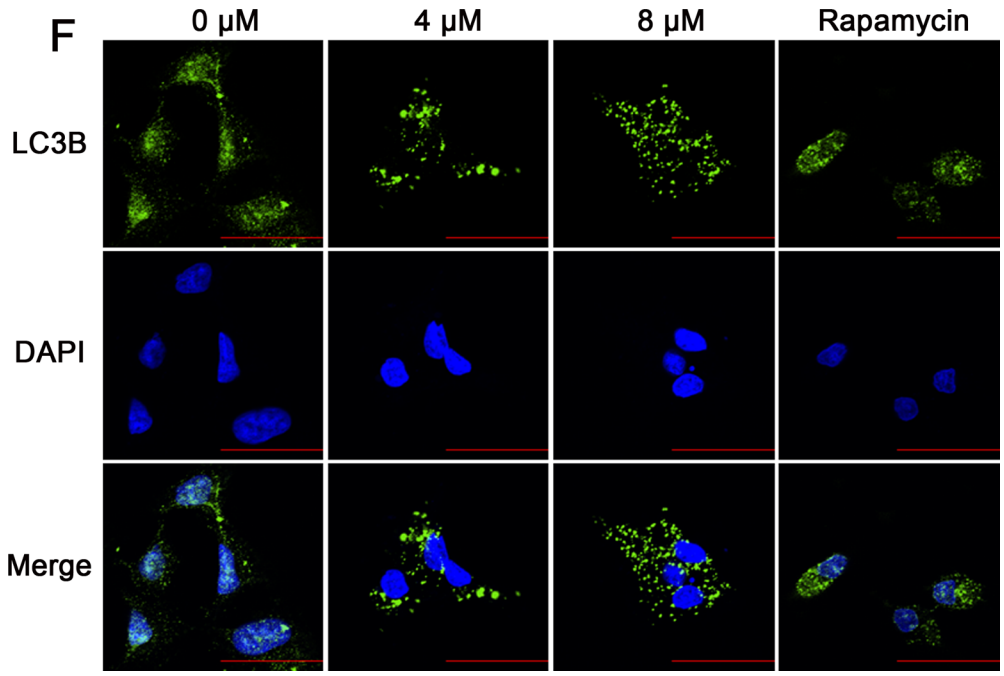


**Fig. 4.** (*continued*)

SDS-PAGE and transferred to 0.22 μm nitrocellulose membranes (Pall, USA). The membrane was blocked with PBS containing 5% skim milk for 2 h at room temperature before incubating overnight with primary antibody diluted in PBST (PBS containing 0.5% Tween-20) at 4 °C. Blots were washed four times in PBST for 5 min each time and then incubated with horseradish peroxidase-conjugated secondary antibody for 2 h at room temperature. The signals were detected after adding the enhanced chemiluminescence (Thermo Fisher Scientific, USA) to blots.

### 2.8. Measurement of the mitochondrial membrane potential

The changes of mitochondrial membrane potential (MMP) was determined using a JC-1 (5,5′6,6′-tetrachloro-1,1′,3,3′-tetraethyl-imidacarbocyanine iodide) assay kit (KeyGen, China). Following collection, the A549 cells were incubated with JC-1 dye staining solution (500 μL) in the dark at 37 °C for 25 min. After that, cells were washed twice with 1 × incubation buffer. Finally, cells were suspended with 500 μL of 1 × incubation buffer and detected by flow cytometry.

### 2.9. Determination of cellular reactive oxygen species (ROS)

DCFH-DA (2′,7′-dichlorofluorescein) could produce a fluorescent compound dichlorofluorescein (DCF) after reacting with ROS. Therefore, it was used to determine the production of intracellular ROS. After exposed to 0.1% DMSO or different concentrations of SO (4, 8 or 12 μM) for 48 h, A549 cells were harvested and incubated with 10 μM DCFH-DA (Beyotime, China) at 37 °C for 20 min in the dark. Fluorescence data was obtained by flow cytometry.

### 2.10. MDC staining

Cells were grown on the coverslips in 6-well plate. After treating with different concentrations of SO for 48 h, the cells were washed with ice-cold PBS and incubated with 50 mM of MDC at 37 °C for 30 min. The stained cells were washed and analyzed by Confocal Microscope with ZEN software. To quantitate MDC, flow cytometry was used. Cells were seeded in 6-well plate. After exposing to various concentrations of SO (4, 8, 12 μM) or DMSO (< 0.1%) for 48 h, the cells were washed with ice-cold PBS, incubated with 50 mM of MDC at 37 °C for 30 min and detected using flow cytometry

### 2.11. Immunofluorescence

A549 cells in confocal laser dish were exposed to different concentrations of SO for 48 h. Cells were fixed with 4% paraformaldehyde at room temperature for 30 min. After that, cells were washed with PBS and blocked with PBS containing 5% BSA for 1 h before incubating overnight with primary antibody against LC3B at 4 °C. Cells were washed with PBS and incubated with Alexa Fluor 488-conjugated secondary antibody (Thermo Fisher Scientific, USA) for 2 h at room temperature in the dark. The nuclei were stained with 5 μg/mL DAPI solution (Solarbio, China) for 10 min prior to obtain image by a laser scanning confocal microscope.

### 2.12. GFP-mCherry-LC3 plasmid and siRNA transient transfection

For siRNA transfection, A549 cells were seeded in 6-well culture plates and transfected by Lipofectamine RNAiMax transfection reagent (Life, USA) in accordance with the manufacturer's instruction. Then, cells were treated with media with or without various concentrations of SO for 48 h and collected for further experiments. For GFP-mCherry-LC3 adenovirus (Hanheng, China) transfection, A549 cells were cultured on a confocal laser dish (Corning, USA). After incubation for 12 h, cells were exposed to SO for 48 h and observed by a confocal microscope.

### 2.13. Statistical analysis

All experiments were done in triplicate. Data were presented as mean ± standard deviation (S.D.). The significance of different groups was determined by one-way or two-way ANOVA and *t*-test. It was considered statistically significant at $p < 0.05$.

## 3. Results

### 3.1. Sanggenon O inhibits the proliferation of A549 cells

To evaluate the anti-proliferative effect of SO (Fig. 1A) on human

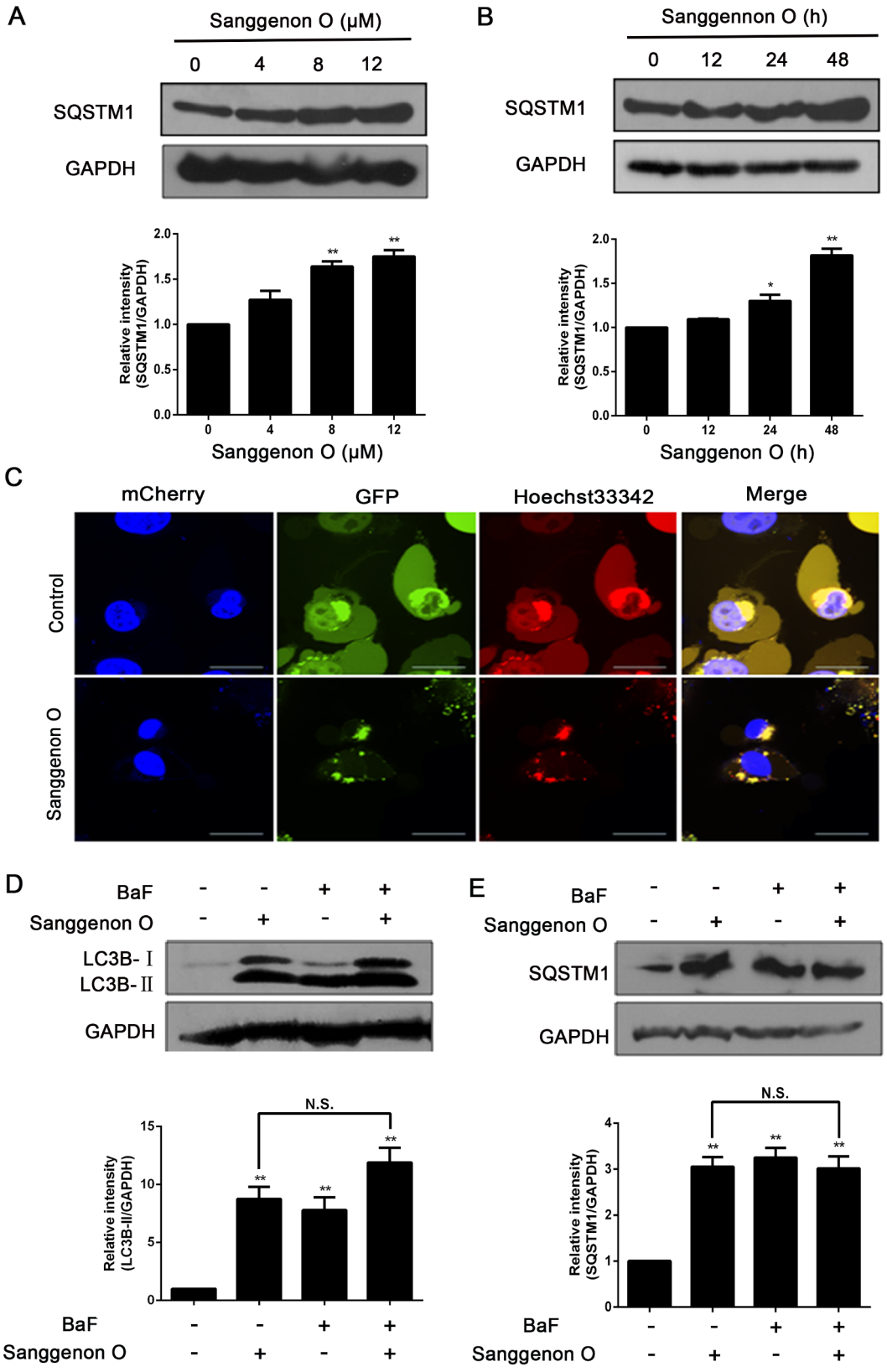


**Fig. 5.** Sanggenon O suppresses autophagic flux in A549 cells. (A and B) After treatment with SO (0–12 μM) for 48 h or SO (8 μM) for various durations (0–48 h), the expression of LC3B-II was analyzed by western blot. (C) After transfected with GFP-mCherry-LC3 adenovirus, the fluorescence was analyzed when A549 cells were treated with 8 μM SO for 48 h. Images were taken by a confocal microcopy (Nikon, Japan). Bar = 20 μm. (D and E) The expressions of LC3B-II and SQSTM1 in A549 cells in the presence or absence of 100 nM BaF (added 12 h before cell harvest) were analyzed by Western blot. $^{*}p < 0.05$ and $^{**}p < 0.01$, compared to control, N.S., not significant.

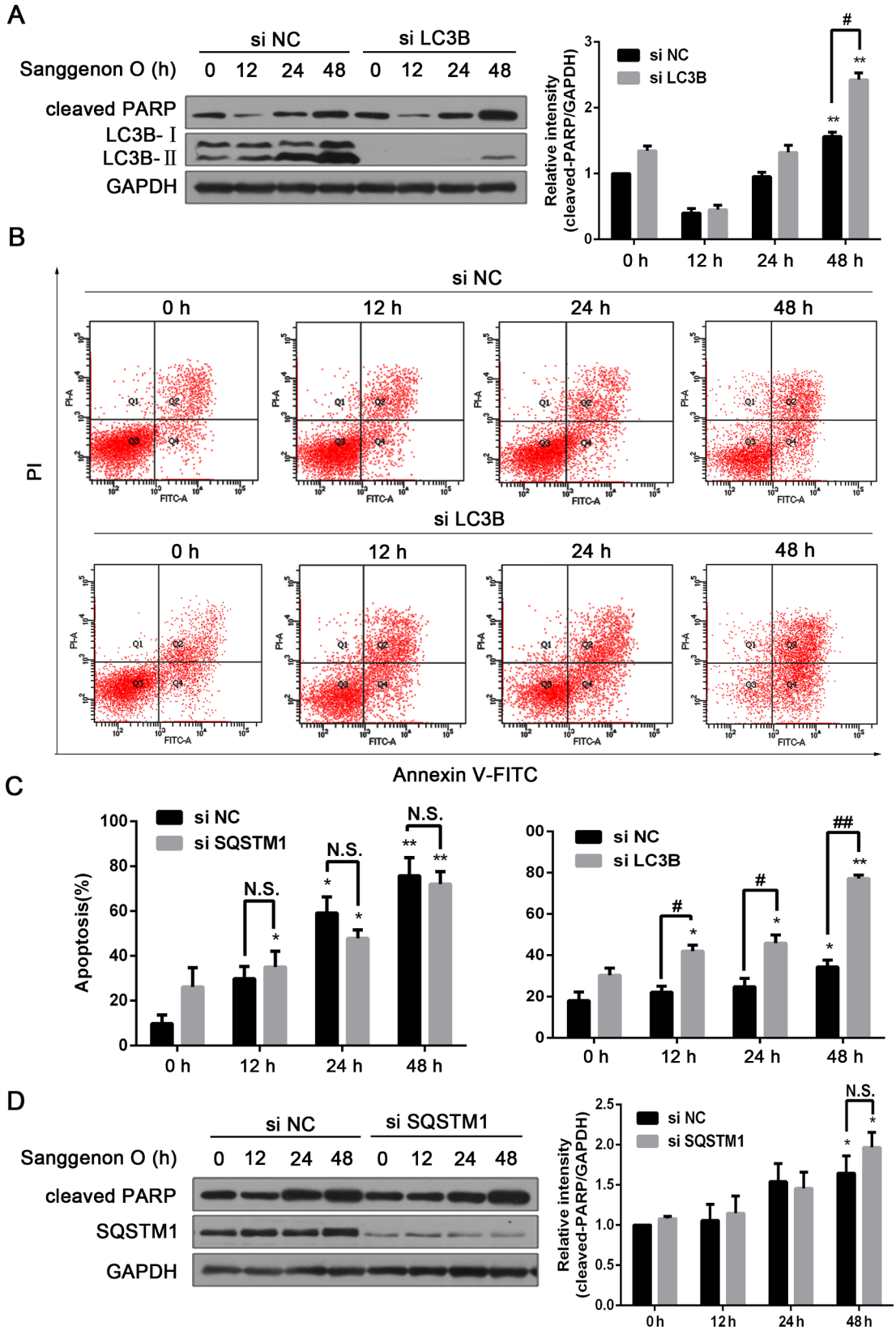


**Fig. 6.** Sanggenon O induces cytoprotective autophagy in A549 cells. (A) The level of cleaved PARP of the LC3B silenced/SO treated A549 cells determined by western blot analysis. (B) Percentages of LC3B silenced/SO treated A549 cells undergoing apoptosis determined by FITC-AV/PI double staining and analyzed by flow cytometry. (C) Percentages of SQSTM1 silenced/SO treated A549 cells undergoing apoptosis determined by AV/PI double staining. (D) The level of cleaved PARP of the SQSTM1 silenced/SO treated A549 cells determined by western blot analysis. GAPDH served as a loading control for all western blot assays. Data are represented as mean ± SD of triple independent experiments. $^{*}p < 0.05$; $^{**}p < 0.01$ and $^{***}p < 0.001$, compared to control. $^{\#}p < 0.05$, $^{\#\#}p < 0.01$ compared to si NC cells at corresponding time by *t*-test, N.S., not significant.

lung cancer cells, A549 cells were treated with a series of concentrations of SO. MTT results showed that SO inhibited the growth of A549 cells (Fig. 1B). Moreover, A549 cells were labeled with CFDA-SE to determine the effect of SO on cell growth. After entering the cells, CFDA-SE was distributed equally to the divided cells with decreased fluorescence intensity. After treatment with SO, the CFDA-SE fluorescence intensity augments in a dose-dependent manner (Fig. 1C), suggesting that SO could inhibit cell division. Next, an EdU incorporation assay was conducted to confirm the inhibitory effect of SO on cell proliferation. Compared with the control group, EdU-positive cells were dramatically decreased in SO treatment groups. (Fig. 1D). Taken together, these results indicated that SO could significantly inhibit the proliferation of human lung carcinoma A549 cells.

### 3.2. Sanggenon O induces mitochondrial dysfunction in human lung cancer A549 cells

Mitochondrial dysfunction is the character of intrinsic apoptosis, resulting in the release of mitochondrial pro-apoptotic factors [17,18]. These molecules lead to the activation of caspase-9 [19], which triggers the catalytic maturation of caspases, such as caspase-3 [20]. In our study, mitochondrial membrane potential (Δ Ψm) was descended in a dose-dependent manner after incubation with SO for 48 h. (Fig. 2A). ROS, generated mainly from mitochondria, could determine the fate of cancer cells by regulating diverse cellular pathways [21]. To evaluate the effect of SO on ROS generation, A549 cells were treated with SO at different concentrations for 48 h. Flow cytometry analysis revealed that ROS increased dose-dependently in SO-treated cells (Fig. 2B). Besides, the Bcl-2 family proteins could also tightly regulate cell apoptosis. Anti-apoptotic proteins such as Bcl-2 could inhibit mitochondrial perturbations [22,23], whereas pro-apoptotic proteins such as Bax could promote the permeabilization of mitochondrial membrane [24–26]. As expected, we observed SO up-regulated the ratio of Bax/Bcl-2 (Fig. 2C). In a word, these results indicated that SO induced mitochondrial dysfunction.

### 3.3. Sanggenon O triggers apoptosis in human lung cancer A549 cells

Annexin V/PI assay was performed to evaluate the apoptotic effect of SO. As shown in Fig. 3A, SO treatments increased the percent of apoptotic cells dose-dependently. Caspase family proteins play an important role in numerous forms of apoptosis [27]. Mitochondrial damage could cleave caspase 9 into an active state, which could activate caspase 3 [28]. So we examined the expression of caspase-related proteins. Fig. 3B and C showed a marked reduction of the proenzymatic, inactive form of caspase-3/7/9/PARP and the concomitant induced cleavage of caspase-3/7/9/PARP by SO treatments in a concentration and time-dependent manner. The above results suggested that SO induced mitochondrion mediated apoptosis in A549 cells.

### 3.4. Sanggenon O induces autophagosome accumulation in human lung cancer A549 cells

Numerous cytoplasmic vacuoles often appeared in cells undergoing autophagy [29,30]. Vacuole bodies appeared in A549 cells when treated with high doses of SO (Fig. 4A). To further assess the effect of SO on autophagy in A549 cells, a series of experiments were carried out. MDC, a tool compound used to stain lysosomes, acidic endosomes and autophagosomes [31], was used to detect acidic vesicular organelles in SO-treated A549 cells. As shown in Fig. 4B, SO-treated A549 cells showed a sharp increase in the amount of MDC-labeled vesicles, demonstrating that SO induces the formation of acidic vesicular organelles, which is a characteristic of autophagy. Consistent with the above results, flow cytometry analysis indicated that SO caused a profound increase in MDC fluorescence intensity in a dose-dependent manner (Fig. 4B and C). During the process of autophagy, the cytoplasmic form LC3B-I is transformed into the lipidated form LC3B-II, which aggregates on the membranes of the autophagosome, thus the level of LC3B-II protein positively correlating with the number of autophagosomes [32]. Therefore, the expression of LC3B-II was detected. As shown in Fig. 4D and E, SO induce the expression of LC3B-II in both dose- and time-dependent manners. Meanwhile, the expression of LC3B-II was determined by immunofluorescence. An increased punctate pattern of LC3B fluorescence was observed in SO-treated A549 cells (Fig. 4F), indicating the formation of autophagic vacuoles and the recruitment of LC3B into autophagosomes. These results indicated that SO induced autophagosome accumulation in A549 cells.

### 3.5. Sanggenon O suppresses autophagic flux in A549 cells

The fusion of autophagosomes and lysosomes is the final step of autophagy [33]. SQSTM1 protein, another autophagy marker, is selectively incorporated into autophagosomes and degraded after autophagy initiation [34]. Therefore, SQSTM1 protein level is expected to increase after inhibiting autophagosome degradation [33]. Fig. 5A and B showed that SO induced SQSTM1 accumulation in a dose- and time-dependent manner. To further explore the effect of SO on autophagy, GFP-mCherry-LC3 adenovirus was transfected in A549 cells. After incubating with SO, a large number of red- and green-fluorescent puncta were formed in transfected cells. These puncta could produce a yellow overlay, which indicated that lysosomes were dysfunctional and the fusion process of autophagosome and lysosome were impaired (Fig. 5C). To further confirm the role of SO in autophagosome accumulation, autophagic flux was determined. BaF, a lysosomotropic inhibitor, can prevent autophagosome degradation by increasing the pH of lysosomal/vacuolar [35]. As shown in Fig. 5D–E, the expressions of LC3B-II and SQSTM1 were not further increased under a dual treatment of SO and BaF. Lysosomal enzymes are necessary for functional lysosomes, so the expressions of LC3B-II and SQSTM1 were also measured under a dual treatment of SO and lysosomal protease inhibitors (CQ or pepstatin A/E64D) [36]. Compared to the cells treated with SO only, the dual treatment of SO and pepstatin A/E64D or CQ did not accumulate SQSTM1 (Fig. S1). The above results indicated that the accumulation of autophagosome induced by SO was related to the inhibition of autophagic degradation.

### 3.6. Sanggenon O induces cytoprotective autophagy in A549 cells

The interaction between autophagy and apoptosis is controversial. In cancer therapy, autophagy induced by agent may be a pro-dead, a protective or an accompanying phenomenon [37,38]. Herein, the functional role of autophagy in SO-induced cytotoxicity was examined. LC3B and SQSTM1, which are critical for autophagosome formation, were knocked down respectively. The SO-induced expression levels of cleaved PARP, a protein marker of apoptosis [39], were increased under siLC3B transfection (Fig. 6A). In addition, the apoptotic rate of SO-treated cells changed from 36.7% to 78.4% after the knockdown of LC3B (Fig. 6B). However, SQSTM1 silencing elicited a subtle effect on cell apoptosis and protein expression levels of c-PARP and c-caspase 3 (Fig. 6C and D). Taken these data together, these results suggested that SO induces protective autophagy in A549 cells.

## 4. Discussion

SO is a flavanone Diel-Alder adduct compound derived from the root bark of *Morus alba* [5]. Previous studies have shown that the structural analogues of SO have cytotoxic activities [13,14]. However, the effect of SO on cancer cells and its anticancer mechanism has not yet been fully clarified. Thus, we investigated the effect of SO on cancer cells. We found that SO could inhibit cell viability in various kinds of human cancer cells (data not shown). In this work, we further verified that SO inhibited cell proliferation, triggered autophagy, and induced

apoptosis via mitochondrial dysfunction in A549 cells. Thus, SO might represent an effective therapeutic agent for the treatment of lung cancer.

Apoptosis one of the most obviously characterized cell death mode, can be induced by two main pathway: the mitochondrial pathway and the death receptor pathway [40]. Numerous natural products induce cell death through the intrinsic apoptosis pathway [41–44]. Similarly, our data demonstrated that SO treatment induced mitochondrial dysfunction by decreasing MMP (Fig. 2A) and increasing reactive oxygen species formation (Fig. 2B). The up-regulation of Bax/Bcl-2 protein expression ratio enhances permeabilization mitochondrial membrane permeabilization which is the main cause of apoptosis [45]. Bax/Bcl-2 protein expression ratios were consistently up-regulated after exposing to SO. All of these findings validate the hypothesis that SO-induced apoptosis is related to mitochondrial dysfunction.

The best character of autophagy encompasses the progressive separation of cytoplasm by autophagosomes, which fuse with lysosomes to initiate the degradation of their contents [46]. Compared with the control group, numerous microscopic vacuoles were observed in A549 cells treated with SO (Fig. 3A), which prompted us to detect the effects of SO on cell autophagy. The autophagic response was confirmed by analysis of MDC labeling. In our results, we found SO treatment increased MDC labeling and fluorescence intensity, suggesting SO induced the occurrence of autophagy. Cleavage of LC3 is another widely used criteria for autophagy. In the process of autophagy, LC3 is cleaved to LC3-II that aggregates and localizes to the autophagosomes [47]. The increased expression of LC3-II was observed in a dose-dependent manner (Fig. 3C). We also found an increased expression of SQSTM1 with SO treatment. To explain this, A549 cells were transfected with GFP-mCherry-LC3 adenovirus and both GFP punctate and mCherry-LC3B fluorescence were increased after SO treatment. This result indicated that the fusion step of autophagosome and lysosome was impaired. The level of SQSTM1 will be increased when the lysosome is dysfunctional or the fusion of lysosomes and autophagosomes is inhibited [44,48–51]. To further prove that the blockage of autophagic degradation is devoted to SO-induced accumulation of autophagosome, other kinds of autophagy flux assays were performed. We found SO-induced cell autophagy was similar to that of other lysosome inhibitors (BaF and pepstatin A/E64D). Taken together, these results indicated that autophagy inhibition was involved in the SO-induced autophagosome accumulation.

Autophagy is a double-edged sword in cancer tumorigenesis and antitumor therapies, hence whether autophagy stimulates cell death or cell survival remains controversial [52]. Therefore, fully understanding of the relationship between cell death and autophagy is significantly important in tumor therapy. Although plenty of drug-induced autophagic cell death has been reported, such as Saikosaponin-d [53], Lapatinib [54] and Baicalein [55], the majority of the autophagic response to numerous chemotherapeutic drugs is cytoprotective [56]. To understand the exact role of autophagy in cell death induced by SO, we assessed the effects of LC3B or SQSTM1 siRNA on SO-induced cell apoptosis respectively. Interestingly, the LC3B genetic inhibition increased SO-induced apoptotic cells and the protein level of cleaved PARP. In summary, SO-triggered apoptosis was enhanced by inhibition of autophagy, indicating that SO-mediated autophagy was a pro-survival mechanism other than a pro-death mechanism in NSCLC cells. It suggested that combination of SO and autophagy inhibitor maybe a promising method for NSCLC therapy.

In conclusion, SO suppressed the proliferation of A549 cells by inducing mitochondrial mediated apoptosis, which was associated with increased Bax/Bcl-2 ratio, leading to a reduce of mitochondrial membrane potential. Moreover, the accumulation of autophagosome plays a protective role in SO-treated cells. Our data identified a novel mechanism by which SO exerts potent anticancer activity. These results indicate that SO possesses great potential to be a promising candidate combined with autophagy inhibitor for the treatment of NSCLC.

## Conflict of interest

The authors declare that they have no conflicts of interest.

## Acknowledgements

This work was supported by National Natural Science Foundation of Youth Fund (No. 81602961, for YCZ); National Natural Science Foundation of China (Project No. 81430085 and No. 21372206 for HML); Outstanding Young Talent Research Fund of Zhengzhou University (No. 1521331002, for YCZ); Key Scientific Research Project for Higher Education by Department of Education of Henan Province He'nan Educational Committee (No. 15A350018, for YCZ); National Key Research Program of Proteins (No. 2016YFA0501800, for HML); Key Research Program of Henan Province (No. 1611003110100, for HML).

## Appendix A. Supplementary material

Supplementary data to this article can be found online at https://doi.org/10.1016/j.bioorg.2019.03.072.

## References

[1] W. Chen, R. Zheng, P.D. Baade, S. Zhang, H. Zeng, F. Bray, A. Jemal, X.Q. Yu, J. He, Cancer statistics in China, 2015, CA Cancer J. Clin. 66 (2016) (2015) 115–132.
[2] W. Chen, R. Zheng, H. Zeng, S. Zhang, The incidence and mortality of major cancers in China, 2012, Chin. J. Cancer 35 (2016) 73–77.
[3] X. Li, X.X. Fan, Z.B. Jiang, W.T. Loo, X.J. Yao, E.L. Leung, L.W. Chow, L. Liu, Shikonin inhibits gefitinib-resistant non-small cell lung cancer by inhibiting TrxR and activating the EGFR proteasomal degradation pathway, Pharmacol. Res. 115 (2017) 45–55.
[4] C. Zhang, L. Yang, X.B. Wang, J.S. Wang, Y.D. Geng, C.S. Yang, L.Y. Kong, Calyxin Y induces hydrogen peroxide-dependent autophagy and apoptosis via JNK activation in human non-small cell lung cancer NCI-H460 cells, Cancer Lett. 340 (2013) 51–62.
[5] R.C. Shen, M. Lin, Diels-Alder type adducts from Morus cathayana, Phytochemistry 57 (2001) 1231–1235.
[6] M. Zhang, M. Chen, H.Q. Zhang, S. Sun, B. Xia, F.H. Wu, In vivo hypoglycemic effects of phenolics from the root bark of *Morus alba*, Fitoterapia 80 (2009) 475–477.
[7] S. Sun, M. Zhang, M. Li, F. Guan, F. Wu, X. Feng, B. Xia, H. Zhang, Compounds inhibiting hyperglycemia and cancer cell proliferation from *Morus alba* L, Planta Med. 78 (2012) 1202.
[8] K.O. Chung, B.Y. Kim, M.H. Lee, Y.R. Kim, H.Y. Chung, J.H. Park, J.O. Moon, In-vitro and in-vivo anti-inflammatory effect of oxyresveratrol from *Morus alba* L, J. Pharm. Pharmacol. 55 (2003) 1695–1700.
[9] Y.C. Chen, Y.J. Tien, C.H. Chen, F.N. Beltran, E.C. Amor, R.J. Wang, D.J. Wu, C. Mettling, Y.L. Lin, W.C. Yang, *Morua alba* and active compound oxyresveratrol exert anti-inflammatory activity via inhibition of leukocyte migration involving MEK/ERK signaling, BMC Complem. Altern. M 13 (2013) 45–54.
[10] T. Katsube, N. Imawaka, Y. Kawano, Y. Yamazaki, K. Shiwaku, Y. Yamane, Antioxidant flavonol glycosides in mulberry (*Morus alba* L.) leaves isolated based on LDL antioxidant activity, Food Chem. 97 (2006) 25–31.
[11] H.A. El-Beshbishy, A.N. Singab, J. Sinkkonen, K. Pihlaja, Hypolipidemic and antioxidant effects of *Morus alba* L. (Egyptian mulberry) root bark fractions supplementation in cholesterol-fed rats, Life Sci. 78 (2006) 2724–2733.
[12] X.K. Zheng, Y.G. Cao, Y.Y. Ke, Y.L. Zhang, F. Li, J.H. Gong, X. Zhao, H.X. Kuang, W.S. Feng, Phenolic constituents from the root bark of *Morus alba* L. and their cardioprotective activity in vitro, Phytochemistry 135 (2017) 128–134.
[13] H. Huang, N. Liu, K. Zhao, C. Zhu, X. Lu, S. Li, W. Lian, P. Zhou, X. Dong, C. Zhao, H. Guo, C. Zhang, C. Yang, G. Wen, L. Lu, X. Li, L. Guan, C. Liu, X. Wang, Q.P. Dou, J. Liu, Sanggenon C decreases tumor cell viability associated with proteasome inhibition, Front. Biosci. 3 (2011) 1315–1325.
[14] L.C. Li, F. Shen, Q. Hou, G.F. Cheng, Inhibitory effect and mechanism of action of sanggenon C on human polymorphonuclear leukocyte adhesion to human synovial cells, Acta Pharmacol. Sin. 23 (2002) 138–142.
[15] W.B. Wang, L.X. Feng, Q.X. Yue, W.Y. Wu, S.H. Guan, B.H. Jiang, M. Yang, X. Liu, D.A. Guo, Paraptosis accompanied by autophagy and apoptosis was induced by celastrol, a natural compound with influence on proteasome, ER stress and Hsp90, J. Cell. Physiol. 227 (2012) 2196–2206.
[16] D.J. Klionsky, S.D. Emr, Autophagy as a regulated pathway of cellular degradation, Science 290 (2000) 1717–1721.
[17] G. van Loo, X. Saelens, M. van Gurp, M. MacFarlane, S.J. Martin, P. Vandenabeele, The role of mitochondrial factors in apoptosis: a Russian roulette with more than one bullet, Cell Death Differ. 9 (2002) 1031–1042.
[18] X. Saelens, N. Festjens, L. Vande Walle, M. van Gurp, G. van Loo, P. Vandenabeele, Toxic proteins released from mitochondria in cell death, Oncogene 23 (2004)

2861–2874.
[19] D. Acehan, X. Jiang, D.G. Morgan, J.E. Heuser, X. Wang, C.W. Akey, Three-dimensional structure of the apoptosome: implications for assembly, procaspase-9 binding, and activation, Mol. Cell 9 (2002) 423–432.
[20] P. Li, D. Nijhawan, I. Budihardjo, S.M. Srinivasula, M. Ahmad, E.S. Alnemri, X. Wang, Cytochrome c and dATP-dependent formation of Apaf-1/caspase-9 complex initiates an apoptotic protease cascade, Cell 91 (1997) 479–489.
[21] M.B. Azad, Y. Chen, S.B. Gibson, Regulation of autophagy by reactive oxygen species (ROS): implications for cancer progression and treatment, Antioxid. Redox Sign. 11 (2009) 777–790.
[22] G. Kroemer, The proto-oncogene Bcl-2 and its role in regulating apoptosis, Nat. Med. 3 (1997) 614–620.
[23] D.T. Chao, S.J. Korsmeyer, BCL-2 family: regulators of cell death, Annu. Rev. Immunol. 16 (1998) 395–419.
[24] G. Kroemer, J.C. Reed, Mitochondrial control of cell death, Nat. Med. 6 (2000) 513–519.
[25] M.G. Vander Heiden, C.B. Thompson, Bcl-2 proteins: regulators of apoptosis or of mitochondrial homeostasis? Nat. Cell Biol. 1 (1999) E209–E216.
[26] A. Letai, M.C. Bassik, L.D. Walensky, M.D. Sorcinelli, S. Weiler, S.J. Korsmeyer, Distinct BH3 domains either sensitize or activate mitochondrial apoptosis, serving as prototype cancer therapeutics, Cancer Cell 2 (2002) 183–192.
[27] P.J. Utz, P. Anderson, Life and death decisions: regulation of apoptosis by proteolysis of signaling molecules, Cell Death Differ. 7 (2000) 589–602.
[28] K.M. Boatright, G.S. Salvesen, Mechanisms of caspase activation, Curr. Opin. Cell Biol. 15 (2003) 725–731.
[29] T. Li, Z.H. Tang, W.S. Xu, G.S. Wu, Y.F. Wang, L.L. Chang, H. Zhu, X.P. Chen, Y.T. Wang, Y. Chen, J.J. Lu, Platycodin D triggers autophagy through activation of extracellular signal-regulated kinase in hepatocellular carcinoma HepG2 cells, Eur. J. Pharmacol. 749 (2015) 81–88.
[30] Z.H. Tang, W.X. Cao, M.X. Su, X. Chen, J.J. Lu, Osimertinib induces autophagy and apoptosis via reactive oxygen species generation in non-small cell lung cancer cells, Toxicol. Appl. Pharma. 321 (2017) 18–26.
[31] D.B. Munafo, M.I. Colombo, A novel assay to study autophagy: regulation of autophagosome vacuole size by amino acid deprivation, J. Cell Sci. 114 (2001) 3619–3629.
[32] N. Mizushima, T. Yoshimori, How to interpret LC3 immunoblotting, Autophagy 3 (2007) 542–545.
[33] A.C. Kimmelman, The dynamic nature of autophagy in cancer, Gene Dev. 25 (2011) 1999–2010.
[34] G. Bjorkoy, T. Lamark, S. Pankiv, A. Overvatn, A. Brech, T. Johansen, Monitoring autophagic degradation of p62/SQSTM1, Method Enzymol. 452 (2009) 181–197.
[35] H.M. Ni, A. Bockus, A.L. Wozniak, K. Jones, S. Weinman, X.M. Yin, W.X. Ding, Dissecting the dynamic turnover of GFP-LC3 in the autolysosome, Autophagy 7 (2011) 188–204.
[36] I. Tanida, T. Ueno, E. Kominami, LC3 and autophagy, Method Mol. Biol. 445 (2008) 77–88.
[37] Z.H. Tang, W.X. Cao, Z.Y. Wang, J.H. Lu, B. Liu, X. Chen, J.J. Lu, Induction of reactive oxygen species-stimulated distinctive autophagy by chelerythrine in non-small cell lung cancer cells, Redox Bio. 12 (2017) 367–376.
[38] Z.H. Tang, L.L. Zhang, T. Li, J.H. Lu, D.L. Ma, C.H. Leung, X.P. Chen, H.L. Jiang, Y.T. Wang, J.J. Lu, Glycyrrhetinic acid induces cytoprotective autophagy via the inositol-requiring enzyme 1alpha-c-Jun N-terminal kinase cascade in non-small cell lung cancer cells, Oncotarget 6 (2015) 43911–43926.
[39] G.M. Cohen, Caspases: the executioners of apoptosis, Biochem. J. 326 (1997) 1–16.
[40] C. Liu, K. Gong, X. Mao, W. Li, Tetrandrine induces apoptosis by activating reactive oxygen species and repressing Akt activity in human hepatocellular carcinoma, Int. J. Cancer 129 (2011) 1519–1531.
[41] X.Z. Wang, Y. Cheng, H. Wu, N. Li, R. Liu, X.L. Yang, Y.Y. Qiu, H.M. Wen, J.Y. Liang, The natural secolignan peperomin E induces apoptosis of human gastric carcinoma cells via the mitochondrial and PI3K/Akt signaling pathways in vitro and in vivo, Phytomedicine 23 (2016) 818–827.
[42] L. Zhao, Q. Wen, G. Yang, Z. Huang, T. Shen, H. Li, D. Ren, Apoptosis induction of dehydrobruceine B on two kinds of human lung cancer cell lines through mitochondrial-dependent pathway, Phytomedicine 23 (2016) 114–122.
[43] K.L. Jian, C. Zhang, Z.C. Shang, L. Yang, L.Y. Kong, Eucalrobusone C suppresses cell proliferation and induces ROS-dependent mitochondrial apoptosis via the p38 MAPK pathway in hepatocellular carcinoma cells, Phytomedicine 25 (2017) 71–82.
[44] Y.D. Geng, C. Zhang, Y.M. Shi, Y.Z. Xia, C. Guo, L. Yang, L.Y. Kong, Icariside II-induced mitochondrion and lysosome mediated apoptosis is counterbalanced by an autophagic salvage response in hepatoblastoma, Cancer Lett. 366 (2015) 19–31.
[45] A.S. Belzacq, H.L.A. Vieira, F. Verrier, G. Vandecasteele, I. Cohen, M.C. Prevost, E. Larquet, F. Pariselli, P.X. Petit, A. Kahn, R. Rizzuto, C. Brenner, G. Kroemer, Bcl-2 and bax modulate adenine nucleotide translocase activity, Cancer Res. 63 (2003) 541–546.
[46] L. Galluzzi, E.H. Baehrecke, A. Ballabio, P. Boya, J.M. Bravo-San Pedro, F. Cecconi, A.M. Choi, C.T. Chu, P. Codogno, M.I. Colombo, A.M. Cuervo, J. Debnath, V. Deretic, I. Dikic, E.L. Eskelinen, G.M. Fimia, S. Fulda, D.A. Gewirtz, D.R. Green, M. Hansen, J.W. Harper, M. Jaattela, T. Johansen, G. Juhasz, A.C. Kimmelman, C. Kraft, N.T. Ktistakis, S. Kumar, B. Levine, C. Lopez-Otin, F. Madeo, S. Martens, J. Martinez, A. Melendez, N. Mizushima, C. Munz, L.O. Murphy, J.M. Penninger, M. Piacentini, F. Reggiori, D.C. Rubinsztein, K.M. Ryan, L. Santambrogio, L. Scorrano, A.K. Simon, H.U. Simon, A. Simonsen, N. Tavernarakis, S.A. Tooze, T. Yoshimori, J. Yuan, Z. Yue, Q. Zhong, G. Kroemer, Molecular definitions of autophagy and related processes, EMBO J. 36 (2017) 1811–1836.
[47] S. Paglin, T. Hollister, T. Delohery, N. Hackett, M. McMahill, E. Sphicas, D. Domingo, J. Yahalom, A novel response of cancer cells to radiation involves autophagy and formation of acidic vesicles, Cancer Res. 61 (2001) 439–444.
[48] G. Kroemer, M. Jaattela, Lysosomes and autophagy in cell death control, Nat. Rev. Cancer 5 (2005) 886–897.
[49] M. Bordi, M.J. Berg, P.S. Mohan, C.M. Peterhoff, M.J. Alldred, S. Che, S.D. Ginsberg, R.A. Nixon, Autophagy flux in CA1 neurons of Alzheimer hippocampus: Increased induction overburdens failing lysosomes to propel neuritic dystrophy, Autophagy 12 (2016) 2467–2483.
[50] H. Zhu, X. Yu, S. Zhu, X. Li, B. Lu, Z. Li, C. Yu, The fusion of autophagosome with lysosome is impaired in L-arginine-induced acute pancreatitis, Int. J. Clin. Exp. Patho. 8 (2015) 11164–11170.
[51] R.E. Varga, M. Khundadze, M. Damme, S. Nietzsche, B. Hoffmann, T. Stauber, N. Koch, J.C. Hennings, P. Franzka, A.K. Huebner, M.M. Kessels, C. Biskup, T.J. Jentsch, B. Qualmann, T. Braulke, I. Kurth, C. Beetz, C.A. Hubner, In vivo evidence for lysosome depletion and impaired autophagic clearance in hereditary spastic paraplegia type SPG11, PLoS Genet. 11 (2015) e1005454.
[52] T. Shintani, D.J. Klionsky, Autophagy in health and disease: a double-edged sword, Science 306 (2004) 990–995.
[53] V.K. Wong, T. Li, B.Y. Law, E.D. Ma, N.C. Yip, F. Michelangeli, C.K. Law, M.M. Zhang, K.Y. Lam, P.L. Chan, L. Liu, Saikosaponin-d, a novel SERCA inhibitor, induces autophagic cell death in apoptosis-defective cells, Cell Death Dis. 4 (2013) e720.
[54] Y.J. Chen, C.W. Chi, W.C. Su, H.L. Huang, Lapatinib induces autophagic cell death and inhibits growth of human hepatocellular carcinoma, Oncotarget 5 (2014) 4845–4854.
[55] P. Aryal, K. Kim, P.H. Park, S. Ham, J. Cho, K. Song, Baicalein induces autophagic cell death through AMPK/ULK1 activation and downregulation of mTORC1 complex components in human cancer cells, FEBS J. 281 (2014) 4458–4644.
[56] Y.L. Hu, A. Jahangiri, M. Delay, M.K. Aghi, Tumor cell autophagy as an adaptive response mediating resistance to treatments such as antiangiogenic therapy, Cancer Res. 72 (2012) 4294–4299.